Valley density-wave and multiband superconductivity in iron-based pnictide superconductors

Vladimir Cvetkovic and Zlatko Tesanovic

Institute for Quantum Matter and Department of Physics & Astronomy, The Johns Hopkins University, Baltimore, Maryland 21218, USA

The key feature of the Fe-based superconductors is their quasi-two-dimensional multiband Fermi surface. By relating the problem to a negative U Hubbard model and its superconducting ground state, we show that the defining instability of such a Fermi surface is the valley density-wave (VDW), a *combined* spin/charge density-wave at the wave vector connecting the electron and hole valleys. As the valley parameters change by doping or pressure, the fictitious superconductor experiences "Zeeman splitting," eventually going into a nonuniform "Fulde-Ferrell-Larkin-Ovchinikov" (FFLO) state, an *itinerant* and often *incommensurate* VDW of the real world, characterized by the metallic conductivity from the ungapped remnants of the Fermi surface. When Zeeman splitting exceeds the "Chandrasekhar-Clogston" limit, the "FFLO" state disappears and the VDW is destabilized. Near this point, the VDW fluctuations and interband pair repulsion are essential ingredients of high-T_c superconductivity in Fe pnictides.

I. INTRODUCTION

Recently, the superconductivity below 7 K in LaOFeP (Ref. 1) led to the discovery of high $T_c \sim 26$ K in its doped sibling LaO$_{1-x}$F$_x$FeAs($x > 0.1$).[2] Even higher T_c's were found by replacing La with other rare earths, up to the current record of $T_c = 55$ K.[3] These are the first noncuprate superconductors (SCs) exhibiting such high T_c's and their discovery has touched off a storm of activity.[4]

In this paper, we introduce a notable element into the theoretical debate by considering a unified model of spin density-wave, orbital density-wave, structural deformation, and superconductivity in Fe pnictides. The model is simple but it contains the necessary physical features. The essential ingredients are electron and hole pockets (valleys) of the quasi-two-dimensional (2D) multiply connected Fermi surface (FS).[5–7] To extract the basic physics we consider spinless electrons first and only a single electron and a single hole band with identical band parameters. We then show that this model can be related to a 2D *negative U* Hubbard model, the ground state of which is known exactly—it is a superconductor.[8] In real FeAs materials, this fictitious superconductivity translates into a fully gapped valley density-wave (VDW), a unified state representing a combination of spin, charge, and orbital density-waves (SDW/CDW/ODW) at the *commensurate* wave vector **M** connecting the two valleys. Next, we introduce two different fictitious "chemical potentials," $\mu^e \neq \mu^h$ for the electron and the hole valleys, as measured from the bottom and the top of the bands, respectively—this describes the effect of doping the parent iron-pnictide compounds and corresponds to the external Zeeman splitting in our fictitious attractive Hubbard model. As $\delta\mu = \mu^e - \mu^h$ increases, so does this Zeeman splitting, and eventually our fictitious superconducting state approaches to and exceeds the "Chandrasekhar-Clogston" limit, giving way to a *nonuniform* Fulde-Ferrell-Larkin-Ovchinikov (FFLO) ground state at an *incommensurate* (IC) wave vector **q**, where $|\mathbf{q}|$ is set by $\delta k_F = k_F^e - k_F^h$, and thus by doping x. This "FFLO state" is nothing but an IC VDW at the wave vector $\mathbf{M} + \mathbf{q}$. Finally, as $\delta k_F(x)$ exceeds certain critical value δk_c

(x_c), the "superconducting" state is completely destroyed and so is the VDW in a true material. However, for δk_F above but near δk_c, we consider strong "superconducting" fluctuations and find that these VDW fluctuations can induce *real* superconductivity in Fe pnictides (see Fig. 1). In principle, one could avoid the mapping to the negative U Hubbard model and argue that the VDW instability in pnictides occurs for the same reasons as the SDW instability found in, say, Cr.[9] We find, however, that our "fictitious superconductivity" description is more appropriate to pnictides not only due to its illustrative purposes but also because it allows us to extend the analogy to the "FFLO" state and multiband "SC," i.e.,
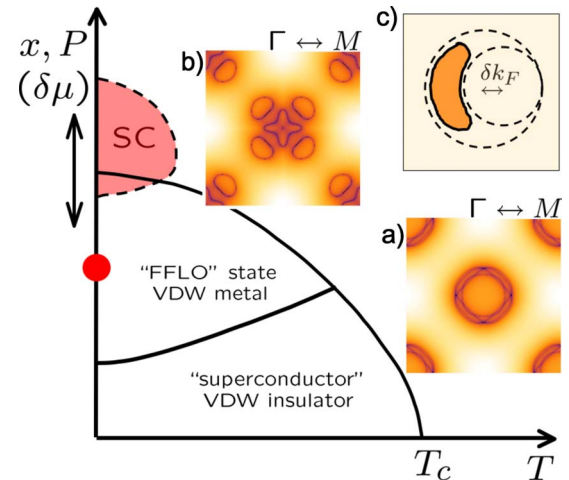

FIG. 1. (Color online) Phase diagram of Fe pnictides, depicting the evolution of our fictitious superconductor from the fully gapped VDW insulator to the "FFLO superconductor"—a partially gapped metallic VDW—to the real SC under the influence of the Zeeman splitting $\delta\mu$ (doping or pressure). The red dot on the vertical axis symbolizes the parent compounds and the regime below it might be physically inaccessible. Insets: FS of (a) the normal state in the folded ($\Gamma \leftrightarrow M$) BZ (Ref. 18), (b) the VDW metal (computed with the interband interaction set to unity)—this is the C_4 version of (c) the continuum FFLO state (Ref. 21). The remaining states are fully gapped.

VDW. Furthermore, the "fictitious superconductor" description allows us to maximize the symmetry of the noninteracting Hamiltonian and classify the interactions by the degree of symmetry breaking they introduce. Finally, it provides a natural venue, by using the known near-rigorous results on two-dimensional superconductors[10] to highlight the crucial role played in real superconductivity by the interband pair-scattering processes, as discussed at length below.

The appearance of an SDW in pnictides along with a structural transition, which we argue to be a signature CDW coupled to phonons, has been established early on in the so-called 1111 family[11] and the universal presence of these orders in other families of pnictides and related materials (122, 11, etc.) has been confirmed by many authors.[12,13] Both the magnetic and the structural order set in at nearly identical temperatures, the experimental fact that has motivated us to model this problem as a one major, "mother" instability (VDW) driven by a large energy scale, which is then split into several stages (say, CDW, followed by SDW, and eventually ODW order) by interaction terms considerably smaller in magnitude. A main feature of our fictitious FFLO state is the ungapped portions of the reconstructed FS(s). These FSs have been observed in pnictides directly[14] as well as indirectly through their signatures in metallic resistivity[15] and recently detected incommensurability of the SDW order.[16]

II. AN IDEALIZED MODEL OF A VALLEY DENSITY-WAVE AND AN FFLO STATE IN A FICTITIOUS SUPERCONDUCTOR

The band structure of Fe pnictides[5–7] can be parametrized by the five-orbital tight-binding model.[17,18] The key feature is the *multiband* nature of the FS, possessing both hole and electron sections. We work with the properly defined Fe-pnictide unit cell which contains two of Fe and two pnictide (As or such) atoms per unit cell. The basic physics is captured by the Hamiltonian describing two hole (c^α) and two electron (d^β) bands centered at the Γ and M points of the 2D Brillouin zone (BZ), respectively,

$$H = H_0 + H_{int}, \qquad (1)$$

$$H_0 = \sum_{\mathbf{k},\sigma,\alpha} \epsilon_{\mathbf{k}}^{(\alpha)} c_{\mathbf{k},\sigma}^{(\alpha)\dagger} c_{\mathbf{k},\sigma}^{(\alpha)} + \sum_{\mathbf{k},\sigma,\beta} \epsilon_{\mathbf{k}}^{(\beta)} d_{\mathbf{k},\sigma}^{(\beta)\dagger} d_{\mathbf{k},\sigma}^{(\beta)}, \qquad (2)$$

$$H_{int} = \frac{1}{2} \int d^2\mathbf{r} d^2\mathbf{r}' V(\mathbf{r},\mathbf{r}') n(\mathbf{r}) n(\mathbf{r}'), \qquad (3)$$

where $\sigma,\sigma' = \uparrow,\downarrow$ and α,β are the spin and band labels, respectively, $\epsilon_{\mathbf{k}}^{(\alpha,\beta)}$ is the hole (electron) dispersion near the FS, $V(\mathbf{r},\mathbf{r}')$ is the effective interaction and $n(\mathbf{r}) = \sum_\sigma \psi_\sigma^\dagger(\mathbf{r}) \psi_\sigma(\mathbf{r})$ with $\psi_\sigma(\mathbf{r}) = \sum_{\mathbf{k},\alpha} c_{\mathbf{k},\sigma}^{(\alpha)} \varphi_{\mathbf{k}}^{(\alpha)}(\mathbf{r}) + \sum_{\mathbf{k},\beta} d_{\mathbf{k},\sigma}^{(\beta)} \phi_{\mathbf{k}}^{(\beta)}(\mathbf{r})$. $\mathbf{k}'$ and $\phi_{\mathbf{k}}^{(\beta)}(\mathbf{r})$ are the Bloch wave functions of hole (electron) bands.

For simplicity, Eq. (3) includes only the screened density-density repulsion; its form becomes more complex if we integrate out the bands away from the Fermi level E_F, generating additional interactions in the spin and interband (orbital) channels. Furthermore, we could equally well start

from the minimal tight-binding representation of Ref. 18 and introduce the interaction term in the Wannier representation as

$$H_{int} = \frac{1}{2} U_d \sum_i n_{di}^2 - J_{\text{Hund}} \sum_i \mathbf{S}_{di}^2 + (\cdots), \qquad (4)$$

where n_{di} and $\mathbf{S}_{di}$ are the total particle number and spin in Wannier d orbitals of iron. U_d describes the overall Hubbard-type repulsion on iron sites while J_{Hund} signifies the intra-d-orbital Hund coupling. In addition, there are numerous intra-d-orbital interactions, as well as various similar terms for p orbitals on pnictide sites, all contributing to $(\cdots)$.[19] However, all such interaction terms feed into the generic classes of quartic vertices near the FS which are generated by H_{int} (3); only the precise numerical values of various vertices are affected. In particular, as long as the influence of J_{Hund} [and $(\cdots)$ terms] is relatively small and one is in the weak-to-intermediate coupling regime argued to be relevant to pnictides,[18] the overall numerical hierarchy of energy scales defined by these various classes of vertices remains intact, as discussed below. Finally, we further simplify the problem by exploiting the fact that all electron (hole) bands have E_F near their bottom (top) and their Fermi wave vectors k_F's are $\ll M$. This allows us to restrict our attention to the first BZ and take continuum limit with $V(\mathbf{r},\mathbf{r}') \to V(\mathbf{r}-\mathbf{r}')$.

H_{int} (3) generates three classes of vertices: (i) the intraband ($c^\dagger c c^\dagger c$ and $d^\dagger d d^\dagger d$), (ii) the interband ($c^\dagger c d^\dagger d$), and (iii) the mixed ($d^\dagger c c^\dagger d$+H.c. and $c^\dagger d c^\dagger d$+H.c.). All arise from $H_{int} \to \frac{1}{2} \sum_\mathbf{q} \widetilde{V}_\mathbf{q} n_\mathbf{q} n_{-\mathbf{q}}$, where

$$n_\mathbf{q} = \sum_{\mathbf{k}\sigma\alpha\alpha'} \zeta_{\mathbf{k+q},\mathbf{k}}^{(\alpha\alpha')} c_{\mathbf{k+q},\sigma}^{(\alpha)\dagger} c_{\mathbf{k},\sigma}^{(\alpha')} + \sum_{\mathbf{k}\sigma\beta\beta'} \zeta_{\mathbf{k+q},\mathbf{k}}^{(\beta\beta')} d_{\mathbf{k+q},\sigma}^{(\beta)\dagger} d_{\mathbf{k},\sigma}^{(\beta')}$$
$$+ \sum_{\mathbf{k}\sigma\alpha\beta} \gamma_{\mathbf{k+q},\mathbf{k}}^{(\alpha\beta)} c_{\mathbf{k+q},\sigma}^{(\alpha)\dagger} d_{\mathbf{k},\sigma}^{(\beta)} + \text{H.c.}, \qquad (5)$$

$\widetilde{V}_\mathbf{q}$ is the Fourier transform of $V(\mathbf{r}-\mathbf{r}')$, and

$$\zeta_{\mathbf{k},\mathbf{k}'}^{(\alpha\alpha')} = \int d^2\mathbf{r} e^{i(\mathbf{k}'-\mathbf{k})\cdot\mathbf{r}} \varphi_{\mathbf{k}}^{(\alpha)*}(\mathbf{r}) \varphi_{\mathbf{k}'}^{(\alpha')}(\mathbf{r}),$$

$$\zeta_{\mathbf{k},\mathbf{k}'}^{(\beta\beta')} = \int d^2\mathbf{r} e^{i(\mathbf{k}'-\mathbf{k})\cdot\mathbf{r}} \phi_{\mathbf{k}}^{(\beta)*}(\mathbf{r}) \phi_{\mathbf{k}'}^{(\beta')}(\mathbf{r}),$$

$$\gamma_{\mathbf{k},\mathbf{k}'}^{(\alpha\beta)} = \int d^2\mathbf{r} e^{i(\mathbf{k}'-\mathbf{k})\cdot\mathbf{r}} \varphi_{\mathbf{k}}^{(\alpha)*}(\mathbf{r}) \phi_{\mathbf{k}'}^{(\beta)}(\mathbf{r}). \qquad (6)$$

The following should be kept in mind about these three classes of vortices: first, all exhibit considerable variation as one moves around the FS. This is the consequence of significant variations in the orbital content of various bands in different portion of the BZ. Second, we find that, generically, the intraband and the interband vertices are comparable in magnitude while the mixed ones are notably smaller. This remains true regardless of whether we use the interaction [Eqs. (3) and (4)] or some other related form as long as J_{Hund} is not dominating the physics and $(\cdots)$ Eq. (4) are relatively small.

To illustrate the latter claim, we include the Hund's coupling to the interaction terms and compare the vertices with and without it. For example, the hole intraband vertex

$$U_{\mathbf{k},\mathbf{k}',\mathbf{q}}^{(\alpha)} c_{\mathbf{k}+\mathbf{q},\sigma}^{(\alpha)\dagger} c_{\mathbf{k}'-\mathbf{q},\sigma'}^{(\alpha)\dagger} c_{\mathbf{k}'\sigma'}^{(\alpha)} c_{\mathbf{k}\sigma}^{(\alpha)} \tag{7}$$

acquires strength

$$U_{\mathbf{k},\mathbf{k}',\mathbf{q}}^{(\alpha)} = \left(V_{\mathbf{q}} + \frac{1}{4}J_{\text{Hund}}\right)\zeta_{\mathbf{k}+\mathbf{q},\mathbf{k}}^{(\alpha\alpha)}\zeta_{\mathbf{k}'-\mathbf{q},\mathbf{k}'}^{(\alpha\alpha)} + \frac{1}{2}J_{\text{Hund}}\zeta_{\mathbf{k}+\mathbf{q},\mathbf{k}'}^{(\alpha\alpha)}\zeta_{\mathbf{k}'-\mathbf{q},\mathbf{k}}^{(\alpha\alpha)} \tag{8}$$

and therefore the Hund's coupling effectively only adds up to the Coulomb potential in this scattering channel. The same is true for other intraband scattering processes, the second mixed term G_2, and most importantly for the interband scattering vertices

$$W_{\mathbf{k},\mathbf{k}',\mathbf{q}}^{(\alpha\beta)} = \left(V_{\mathbf{q}} + \frac{1}{4}J_{\text{Hund}}\right)\zeta_{\mathbf{k}+\mathbf{q},\mathbf{k}}^{(\alpha\alpha)}\zeta_{\mathbf{k}'-\mathbf{q},\mathbf{k}'}^{(\beta\beta)} + \frac{1}{2}J_{\text{Hund}}\gamma_{\mathbf{k}+\mathbf{q},\mathbf{k}'}^{(\alpha\beta)}\gamma_{\mathbf{k},\mathbf{k}'-\mathbf{q}}^{(\alpha\beta)*}, \tag{9}$$

where the second term is negligible for small $\mathbf{q}$. The only interaction vertex that is more affected by J_{Hund} than the others is the first mixed term

$$G_{1/\mathbf{k},\mathbf{k}',\mathbf{q}}^{(\alpha\beta)} = \left(V_{\mathbf{q}} + \frac{1}{4}J_{\text{Hund}}\right)\gamma_{\mathbf{k}+\mathbf{q},\mathbf{k}}^{(\alpha\beta)}\gamma_{\mathbf{k}',\mathbf{k}'-\mathbf{q}}^{(\alpha\beta)*} + \frac{1}{2}J_{\text{Hund}}\zeta_{\mathbf{k}+\mathbf{q},\mathbf{k}}^{(\alpha\alpha)}\zeta_{\mathbf{k}'-\mathbf{q},\mathbf{k}'}^{(\beta\beta)} \tag{10}$$

due to the relative size of ζ's and γ's. However, as long as the screened Coulomb potential is the strongest interaction (i.e., $J_{\text{Hund}} \lesssim V_{\mathbf{q}}$ here) the changes to vertices due to the other sources of scattering [such as those in Eq. (4)] will be only quantitative in nature.

We now observe that the shapes of different sections of the FS (Fig. 1) resemble each other to a reasonable degree. Furthermore, various masses are also roughly similar.[17,18] Thus, to make theoretical progress, it is useful to first assume that all electron and hole bands are equal $-\epsilon_{\mathbf{k}}^{(\alpha=h1)} = -\epsilon_{\mathbf{k}}^{(\alpha=h2)} = \epsilon_{\mathbf{k}+\mathbf{M}}^{(\beta=e1)} = \epsilon_{\mathbf{k}+\mathbf{M}}^{(\beta=e2)} \equiv \epsilon_{\mathbf{k}}^0$. After making the particle-hole (ph) transformation $d_{\mathbf{k},\sigma}^{(\alpha)} \to e_{\mathbf{k},\sigma}^{(\alpha)}$ and $c_{\mathbf{k},\sigma}^{(\alpha)} \to \sigma h_{\mathbf{k},-\sigma}^{(\alpha)\dagger}$, Hamiltonian (1) becomes

$$H_{\text{SU}(8)} \to \sum_{\mathbf{k},\sigma\mu} \epsilon_{\mathbf{k}}^0 \Psi_{\mathbf{k},\sigma}^{(\mu)\dagger} \Psi_{\mathbf{k},\sigma}^{(\mu)} + H_{int}', \tag{11}$$

where $\Psi^{(\mu)\dagger} = (e_1^\dagger, e_2^\dagger, h_1^\dagger, h_2^\dagger)$. Ignoring the effects of bands away from the FS, the kinetic part of $H_{\text{SU}(8)}$ (11) has an exact SU(8) symmetry involving orbital (*both* electron and hole) and spin degrees of freedom, μ and σ, respectively. This symmetry can be used to classify various vertices in H_{int}'—ultimately generated by H_{int} (3) which itself has only $U(1)_{\text{charge}} \times SU(2)_{\text{spin}}$ symmetry—and analyze various symmetry-breaking patterns, starting with $\text{SU}(8) \to \text{SU}(4) \times \text{SU}(4)$, as discussed in Ref. 20.

To illustrate the physics, we focus first on the *minimal* model: $\text{SU}(8) \to \text{SU}(2)$. This leaves one with only two fermion flavors, e and h. Note that *spin* SU(2) symmetry is suppressed but the *orbital* electron-hole symmetry remains as it is essential for this problem. We now obtain

$$H_{\text{SU}(2)} = \sum_{\mathbf{k}} \epsilon_{\mathbf{k}}[e_{\mathbf{k}}^\dagger e_{\mathbf{k}} + h_{\mathbf{k}}^\dagger h_{\mathbf{k}}] + \frac{1}{2}\int d^2\mathbf{r}\,d^2\mathbf{r}'$$
$$\times [U^e(\mathbf{r} - \mathbf{r}')n^e(\mathbf{r})n^e(\mathbf{r}') + U^h(\mathbf{r} - \mathbf{r}')n^h(\mathbf{r})n^h(\mathbf{r}')$$
$$- 2W(\mathbf{r} - \mathbf{r}')n^e(\mathbf{r})n^h(\mathbf{r}')] + H_{\text{SU}(2)}^{\text{mixed}}, \tag{12}$$

where $U^{e/h}(\mathbf{r})$ and $W(\mathbf{r})$ are the Fourier transforms of $\tilde{V}_{\mathbf{k}-\mathbf{k}'}\langle\zeta_{\mathbf{k},\mathbf{k}'}^{(e/h)}\zeta_{\mathbf{k}',\mathbf{k}}^{(e/h)}\rangle_{\text{FS}}$ and $\tilde{V}_{\mathbf{k}-\mathbf{k}'}\langle\zeta_{\mathbf{k},\mathbf{k}'}^{(e)}\zeta^{(h)}(\mathbf{k}',\mathbf{k})\rangle_{\text{FS}}$, respectively. $\langle\cdots\rangle_{\text{FS}}$ indicates the $\mathbf{k}$ and $\mathbf{k}'$ dependence was replaced by the average over the FS—this is justified later. The SU(2) symmetry implies $U^e(\mathbf{r}) = U^h(\mathbf{r})$. Finally, the general H^{mixed} contains smaller mixed vertices and eventually plays a prominent role in our theory; however, we initially—but only temporarily—set it to zero, $H_{\text{SU}(2)}^{\text{mixed}} \to 0$.

The intraband scattering $W(\mathbf{r})$ has a minus sign in front of it. This is the result of the ph transformation and indicates that, we having started with a (screened) Coulomb repulsion between the original electrons, the e and h flavors now mutually *attract*. Consequently, at low energies, $H_{\text{SU}(2)}$ (without $H_{\text{SU}(2)}^{\text{mixed}}$) is *equivalent* to the negative U Hubbard model at low (or high) x, assuming that $W(\mathbf{r})$ is short ranged and $\epsilon_{\mathbf{k}}$ can be represented in the effective-mass approximation [$W(\mathbf{r}) \to W\delta(\mathbf{r})$ and $\epsilon_{\mathbf{k}} \to \mathbf{k}^2/2m$]. Both assumptions should be valid since $k_F \ll M$. The ground state is a "superconductor" with an anomalous correlator $\langle e^\dagger h^\dagger \rangle \neq 0$, where $e^\dagger(h^\dagger)$ creates a "spin-up (down)" fermion $f_\uparrow(f_\downarrow)$. For $T > T_c \sim E_F \exp[-1/N(0)W]$, the system is in its normal state (see phase diagram in Fig. 1). At $T < T_c$ one enters a broken-symmetry state, with "off-diagonal" long-range order and gapped fermions.

Of course, the above "superconductivity" is useful but entirely fictitious mathematical construct, resulting from the ph transformation used to enhance the symmetry of our basic model for iron pnictides. Still, what is this "superconductivity" in the real world? By retracing our steps and undoing the ph transformation, the "off-diagonal" order in $\langle f_{\mathbf{k}\uparrow}^\dagger f_{-\mathbf{k}\downarrow}^\dagger \rangle = \langle e_{\mathbf{k}}^\dagger h_{-\mathbf{k}}^\dagger \rangle$ translates into the diagonal density-wave, $\langle d_{\mathbf{k}+\mathbf{M}}^\dagger c_{\mathbf{k}} \rangle \neq 0$, connecting electrons from two pockets of the FS separated by $\mathbf{M} = (\pi, \pi)$; a VDW. Note that the VDW describes both spin *and* charge/orbital density-waves. With the spin SU(2) symmetry suppressed in our minimal model, one cannot—and should not—distinguish between the two. We identify the above VDW (SDW/CDW/ODW combination) formation as the physical mechanism driving the density-wave orderings observed in numerous experiments.

We can pursue this VDW-"superconductor" analogy a bit further: in real FeAs materials, the electron-hole pockets are not identical, the main difference being their distinct k_F's. In our fictitious superconductor, this translates to different "chemical potentials", $\mu^e \neq \mu^h$ for the electron and the hole valleys. This is nothing but the external Zeeman splitting in a fictitious negative U Hubbard model. As $\delta\mu = \mu^e - \mu^h$ grows, the "superconducting" state approaches the "Chandrasekhar-Clogston" limit, giving way to a nonuniform FFLO ground state at an incommensurate wave vector $\mathbf{q}$, where $|\mathbf{q}|$ is set by $\delta k_F = k_F^e - k_F^h$. This "FFLO state" is just an IC VDW at the wave vector $\mathbf{M} + \mathbf{q}$. Finally, as $\delta k_F(x)$ exceeds certain critical

value $\delta k_c \ (x_c)$, the "superconducting" state is destroyed and so is the VDW (SDW/CDW) in a real FeAs system (Fig. 1).[22]

III. VALLEY DENSITY-WAVE AND INTERBAND SUPERCONDUCTIVITY

The above "superconductor" analysis dealt with an idealized model but its main conclusions apply to the real Fe pnictides: (i) the dominant instability is the VDW at wave vector **M**, a unified spatially modulated state manifested through the *combined* SDW/CDW/ODW and a structural transformation,[11] the details of which depend on nonuniversal features of individual materials; (ii) since hole and electron valleys are not identical, the VDW is the ph analog of a fictitious FFLO state, resulting almost always in portions of the FS which are *not gapped* (Fig. 1). Consequently, the SDW/CDW/ODW's in FeAs are highly itinerant and coexist with finite density of normal charge carriers, exhibiting metallic conductivity;[15] and, finally, (iii) Hamiltonian $H_{\mathrm{SU(2)}}$ (12) *without* the mixed vertices (i.e., with $H_{\mathrm{SU(2)}}^{\mathrm{mixed}} \to 0$) contains only *three* basic ground states: fictitious uniform and nonuniform FFLO "superconductor" (commensurate and incommensurate VDW) and the normal state (Fig. 1). Thus, if purely electronic interactions are to have a prominent role in generating Fe-based superconductivity of the real world, this effect *must* arise from $H_{\mathrm{SU(2)}}^{\mathrm{mixed}}$. This is an important result and an added benefit of our transforming the original problem into a fictitious "superconductor".[10]

With this last point in mind, we now restore these mixed vertices to investigate the real superconductivity in our fictitious "superconductor" model. It is beneficial at this stage to add extra two flavors to the elementary SU(2) model and demand an additional global SU(2) isospin symmetry with respect to these flavors—this isospin degree of freedom is completely inert and can be thought of as either the real spin or an additional orbital index. Its role is purely mathematical as it couches the following analysis in the language most easily translated to the ultimate realistic description of pnictides.[23] Furthermore, viewing this isospin as simply the real spin is useful since, assuming a reasonable degree of total spin conservation in pnictides, the additional SU(2) global symmetry limits the number of terms in H^{mixed} that need to be considered. The mixed vertices allowed by this extension of our model are mixed scattering G_1 and Josephson-type term G_2 which, in absence of nonlocal interactions, has to be in a spin-singlet channel

$$H_{\mathrm{spin}}^{\mathrm{mixed}} \sim G_1 c_\sigma^\dagger d_\sigma d_{\sigma'}^\dagger c_\sigma + \frac{1}{2} G_2 (\sigma c_\sigma^\dagger c_{-\sigma}^\dagger)(\sigma' d_{-\sigma'} d_{\sigma'}) + \mathrm{H.c.} \tag{13}$$

The relation of these vertices to the screened Coulomb interaction is given in Eq. (10). We assume that the corresponding coupling constants are in the regime $G_1, G_2 \ll W, U_h, U_e$, as will be justified momentarily.

These preliminaries in place, we are ready to answer the key question: what is the effect of finite G_1 and G_2 on the previous analysis? Analyzing corrections in the perturbation

theory to our four point vertices, we find contributions to the processes which are dependent on whether the incoming and outgoing spins are parallel or not. This occurs due to the fact that incoming or outgoing states of mixed term G_2 as well as the intraband interaction U are spin singlets of either holes or electrons, Eq. (13). The interband scattering term is therefore conveniently split into two pieces

$$W d_{\sigma'}^\dagger c_\sigma^\dagger c_\sigma d_{\sigma'} \to W' d_{-\sigma}^\dagger c_\sigma^\dagger c_\sigma d_{-\sigma} + W'' d_\sigma^\dagger c_\sigma^\dagger c_\sigma d_\sigma \tag{14}$$

with the bare values for both coupling being identical to W. The first mixed term G_1 is split in identical fashion while the intraband scattering and the G_2 mixed term are required to scatter particles with incoming opposite spins and therefore do not need to undergo the same separation (or equivalently, $G_2'' \equiv 0$, etc.). At the lowest order, we find that different types of vertices receive the following corrections in the perturbation theory:

$$g_U(\omega) = g_U - g_U^2 \ln\left(\frac{\Lambda}{\omega}\right)_{pp} - g_2^2 \ln\left(\frac{\Lambda}{\omega}\right)_{pp},$$

$$g_2(\omega) = g_2 - 2 g_2 g_U \ln\left(\frac{\Lambda}{\omega}\right)_{pp} + 2 g_2 g_W' \ln\left(\frac{\Lambda}{\omega}\right)_{ph}^c$$
$$+ 2 g_2 g_W'' \ln\left(\frac{\Lambda}{\omega}\right)_{ph}^v - 2 g_2 g_1'' \ln\left(\frac{\Lambda}{\omega}\right)_{ph},$$

$$g_W'(\omega) = g_W' + (g_W')^2 \ln\left(\frac{\Lambda}{\omega}\right)_{ph} + g_2^2 \ln\left(\frac{\Lambda}{\omega}\right)_{ph},$$

$$g_W''(\omega) = g_W'' + (g_W'')^2 \ln\left(\frac{\Lambda}{\omega}\right)_{ph},$$

$$g_1'(\omega) = g_1' - 2 g_1' g_1'' \ln\left(\frac{\Lambda}{\omega}\right)_{ph} + 2 g_1' g_W'' \ln\left(\frac{\Lambda}{\omega}\right)_{ph}^v,$$

$$g_1''(\omega) = g_1'' - (g_1')^2 \ln\left(\frac{\Lambda}{\omega}\right)_{ph} - (g_1'')^2 \ln\left(\frac{\Lambda}{\omega}\right)_{ph}$$
$$- g_2^2 \ln\left(\frac{\Lambda}{\omega}\right)_{ph} + 2 g_1'' g_W'' \ln\left(\frac{\Lambda}{\omega}\right)_{ph}^v, \tag{15}$$

where g_U, g_2, g_W', g_W'', g_1', and g_1'' are just the vertices $U(=U_h=U_e)$,[23] G_2, W', W'', G_1', and G_1'', respectively, measured in units of inverse density of states at the Fermi level. The logarithmic divergences in Eq. (15) arise from two sources: first, the standard Cooper pairing instability in the particle-particle (pp) channel and second, the perfect nesting of the hole and electron bands in the particle-hole (ph) channel, i.e., our fictitious "Cooper" instability. Finally, $\ln(\frac{\Lambda}{\omega})_{ph}^{c(v)}$ denotes a crossing (vertex) diagram in the ph channel—it strictly diverges only in the $k_F^{e,h}/M \to 0$ limit and is otherwise finite. Needless to say, there are many additional terms that contribute to various vertices at the leading order in perturbation theory. However, all such terms are finite in the low energy limit and are omitted from Eq. (15).

The third and fourth lines of Eq. (15) are just the mathematical shorthand for our earlier discussion: under renor-
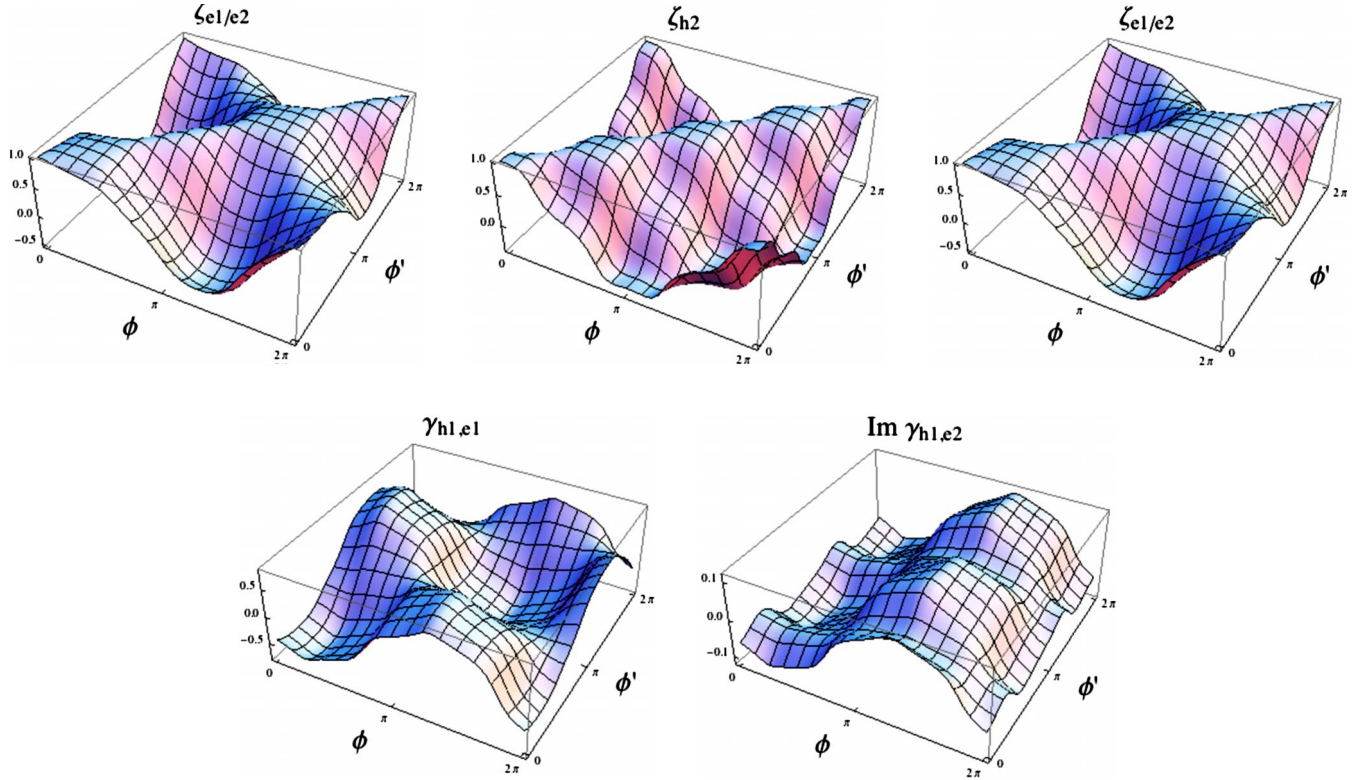
FIG. 2. (Color online) (a) Inter/intraband $\zeta_{\mathbf{k},\mathbf{k}'}^{(e/h)}$ of Eq. (5) (in $k_F \ll M$ limit) for the inner and outer hole bands, and the electron bands as $\mathbf{k}$ and $\mathbf{k}'$ go around respective FSs. (b) Mixed $\gamma_{\mathbf{k},\mathbf{k}'}^{(e,h)}$ Eq. (5) are clearly smaller than ζ's.

malization, the coupling constants g_W' and g_W'' keep growing, ultimately generating the VDW instability, driven by W (the short-ranged attraction of our fictitious Hubbard model). We notice, however, that G_2 enhances the growth of W', thereby giving slight edge to SDW (spin triplet) over a CDW (spin singlet). The first and last two lines tell us that U and G_1's do not interfere: the intraband repulsion g_U, initially large, is rapidly renormalized downwards, toward the Fermi-liquid behavior. g_1's are typically small to begin with and are also driven down; in practice, they can be set to zero. The interesting physics is reserved for G_2. The growth of g_W's fuels the growth of g_2 and thus the mixed vertex describing the resonant pair scattering between the hole and electron bands—i.e., the "Josephson" interband vertex $c^\dagger d c^\dagger d$ +H.c.—becomes strongly enhanced as one approaches the VDW (SDW/CDW/ODW) instability. However, since typically $G_2 \ll W$ (see below), g_W wins, resulting in the VDW order. Once the VDW is formed, the fermions are gapped and the singular behavior disappears, and with it any additional enhancement of G_2.

The situation changes, however, when the differences in size between h and e bands are included, i.e., when the "Zeeman splitting" is turned on, by doping or pressure in real FeAs (Fig. 1). This cuts off the fictitious "Cooper" divergence, resulting in our "FFLO" state and eventual disappearance of VDW. In this case, the portions or even all of the FS is still available for the true Cooper pairing and the real superconductivity becomes a viable option. The remarkable feature of interband pair resonance is that it can produce real superconductivity *irrespective* of its sign.[24] Thus, strongly enhanced G_2 can take advantage of the real-world Cooper singularity—which is always present—and amplify a preexisting *intraband* superconducting instability or generate one entirely on its own. We will revisit this point shortly.

IV. VALLEY DENSITY-WAVE AND SUPERCONDUCTIVITY IN REAL IRON PNICTIDES

This is as far as we can go within the idealized picture: we now must face up to the complexities of the real materials. First, there are four, two h and two e, bands which deviate from an ideal parabolic shape and whose k_F's are different and second, all vertices—intraband, interband, and mixed—have considerable structure as one moves over different portions of the FS. The latter is an important point and reflects a fundamental feature of FeAs: all five d orbitals need to be included in realistic calculations and various two-orbital and three-orbital models will fall short in addressing the phenomenology of real materials. We find that, no more than a single orbital, $d_{2z^2-x^2-y^2}$, can be dropped without a major qualitative disruption of the character of the electronic states at the FS; thus a four-orbital description is the absolute minimum. Finally, the lattice effects produce modifications to our continuum picture which need to be addressed.[22]

We use the full $8+8$-band tight-binding model[18] to find the electron ($\varphi_{\mathbf{k}}^{(\alpha)}$) and hole ($\phi_{\mathbf{k}}^{(\beta)}$) wave functions. This model yields ζ's and γ's Eq. (5) shown in Fig. 2. For a fixed

$\mathbf{k}$, a given ζ varies as $\mathbf{k}'$ goes around the FS. At $\mathbf{k}=\mathbf{k}'$, the normalization of wave-function sets ζ to 1. As $\mathbf{k}$ and $\mathbf{k}'$ move apart, so does ζ decreases until it reaches its minimum at $\mathbf{k}'=-\mathbf{k}$. Based on the symmetry properties of the atomic orbitals, one obtains ($k_F \ll M$)

$$\zeta_{\mathbf{k},-\mathbf{k}}^{(\alpha)} = \pm \left(\sum_{\mu \in even} |b_\mu^{(\alpha)}|^2 - \sum_{\mu \in odd} |b_\mu^{(\alpha)}|^2 \right), \qquad (16)$$

where $b_\mu^{(\alpha)}$ is the amplitude of atomic orbital μ in a hole state (α) or, equivalently, an electron state (β). Each orbital's contribution is determined by its in-plane parity [i.e., sign change under $(x,y,z) \rightarrow (-x,-y,z)$]; even/odd orbitals contribute with $+/-$ or vice versa. Our model uses orbitals of different parity, and consequently, Eq. (16) is bound between -1 and 1, the precise value depending on the amount of mixing of even and odd orbitals within a state. For example, compare $\zeta^{(h1)}$ and $\zeta^{(h2)}$ (Fig. 2). Since both hole bands have a significant contribution of $d_{xz/yz}$ atomic orbitals (odd), both are similarly shaped. The fourfold repetitive structure is due to the C_4 lattice symmetry. However, the minimum values ($\mathbf{k}=-\mathbf{k}'$) are different: $\zeta^{(h1)}$ nearly reaches -1, whereas $\zeta^{(h2)} \gtrsim -0.6$. This reflects the fact that the outer hole band possess a significant overlap with d_{xy} (even) orbital state while the inner hole band is almost entirely made of odd bands. In a more limited model, where only bands of a certain parity are kept,[25] a topological "Berry phase winding" can be defined for each section of the FS.[26] Depending on this "winding," $\zeta_{\mathbf{k},-\mathbf{k}}$ would have to be either $+1$ or -1 and the consequences of the latter would include a suppression of an s-wave VDW in the favor of a p-wave one. Within our model, this notion of topology is absent.

Next, the above form factors ζ's and γ's are used to compute all the interaction vertices (intraband, interband, and mixed) stemming from Eq. (3) along different sections of the FS ($h1$, $h2$, $e1$, and $e2$) and to extract the corresponding coupling constants in the C_4 "angular momentum" channels, s, p, and d. The results, normalized by the overall strength of the screened Coulomb interaction in Eq. (3), are

	U				W			
	$(h1)$	$(h2)$	$(e1)$	$(e2)$	$(h1,e1)$	$(h1,e2)$	$(h2,e1)$	$(h2,e2)$
s	0.44	0.31	0.36	0.35	0.21	0.25	0.27	0.29
p_x	0.02	0.10	0.08	0.10	0.11	0.10	0.11	0.11
p_y	0.02	0.10	0.09	0.10	0.11	0.10	0.11	0.11
$d_{x^2-y^2}$	0.14	0.08	0.02	0.03	0.06	0.07	0.05	0.06
d_{2xy}	0.08	0.04	0.07	0.07	0.05	0.06	0.04	0.05

$$(17)$$

	G_1				G_2			
	$(h1,e1)$	$(h1,e2)$	$(h2,e1)$	$(h2,e2)$	$(h1,e1)$	$(h1,e2)$	$(h2,e1)$	$(h2,e2)$
s	0.11	0.00	0.00	0.00	0.15	0.01	0.11	0.02
p_x	0.00	0.00	0.00	0.00	0.00	0.00	0.01	0.00
p_y	0.00	0.00	0.00	0.00	0.00	0.00	0.01	0.00
$d_{x^2-y^2}$	0.00	0.00	0.04	0.00	0.00	0.00	0.00	0.00
d_{2xy}	0.05	0.00	0.00	0.00	0.03	0.00	0.00	0.00

$$(18)$$

All the vertices [Eqs. (17) and (18)] are given in the original c and d electron basis (1–3) and are all positive (repulsive); they are easily converted into the basis used in Eq. (11) by the ph transformation (i.e., $W \rightarrow -W$, etc.). The numbers in the above table change if additional forms of interaction in real space are considered, for example, those of Eq. (4), as discussed earlier. Again, provided one is outside the regime dominated by the Hund's coupling, such changes are minor.

Obviously, when it comes to the interband vertex (W) as well as all the other vertices, the "s-wave" channel dominates, which retroactively justifies our earlier idealized analysis in terms of an attractive Hubbard model and a fictitious "superconductor". We find that—depending on the overall strength of Coulomb repulsion—the most likely ground state is a multiband VDW (SDW/CDW/ODW) which, due to the mismatch of the hole and electron bands and the underlying lattice effects, is generically in the "FFLO" region of the phase diagram in Fig. 1, leaving portions of the original FS ungapped and metallic. As expected, this VDW (SDW/CDW/ODW) symmetry breaking at wave vector $\mathbf{M}$ is fueled by a large susceptibility of nearly nested hole and electron valleys.[18]

If the Coulomb repulsion is just below what is needed to produce a metallic VDW (Fig. 1), the mixed Josephson vertex G_2 is strongly enhanced, as illustrated by Eq. (15) and surrounding discussion. This is the regime where the inter-

band superconductivity[6,18,27] is possible. Here, an important point needs to be made: there are *two* ways in which G_2 can lead to high-temperature superconductivity in Fe pnictides: first, G_2 *itself* can be *the source* of superconductivity. This is a naturally appealing theoretical scenario since it relies on the proximity to a VDW (SDW) instability to enhance G_2 and uses purely electronic interactions to generate superconducting order. The difficulty in this case is that G_2 has to overwhelm the intraband Coulomb repulsion U^e and U^h before superconductivity becomes possible, the condition being roughly $G_2 > \sqrt{U^e U^h}$. While G_2 takes off as one approaches the VDW (SDW/CDW/ODW), there is a reflection of this enhancement in the renormalized values of U^e and U^h as well. For the realistic model with four inequivalent bands and the interaction vertices displayed in Eqs. (17) and (18), this balancing act between U's and G_2 becomes very sensitive, particularly since the bare U's start as generically larger and only two of G_2's are not negligible in size while all four U's are appreciable. Any effort to extend Eq. (15) to four realistic bands and to all (intraband, interband, and mixed) vertices quickly descends into impenetrable numerics with the above sensitivity to the bare values in Eqs. (17) and (18), making it difficult to reach firm quantitative conclusions. A notable recent progress along these lines was made in Ref. 28.

However, there is a reasonably straightforward way to illustrate the *qualitative* argument for the interband superconductivity mechanism near the VDW phase boundary. This argument follows straight from Eq. (15). Imagine that our isospin label is simply an ordinary spin. Therefore, we have spinful electrons with two (instead of four in real pnictides) orbital flavors, c and d (h and e). In this case, G_2 is the interband pairing resonance in the spin-singlet channel. As argued earlier, we can safely set $G_1 = 0$ and rewrite the remaining parts of Eq. (15) as

$$\dot{g}_U = -g_U^2 - g_2^2,$$

$$\dot{g}_W' = (g_W')^2 + g_2^2,$$

$$\dot{g}_W'' = (g_W'')^2,$$

$$\dot{g}_2 = -2g_2 g_U + 2g_2(g_W' + g_W''), \tag{19}$$

where g's are functions of $\ln(\frac{\Lambda}{\omega})$ and $\dot{g} \equiv dg/d\ln(\frac{\Lambda}{\omega})$ and we again assume $U_h = U_e = U$.

Imagine for the moment that there is no last term in the last line of Eq. (19), i.e., W's and G_2 are not directly coupled. As one moves to low energies $\omega \to 0$, g_W's rapidly grow and one ultimately reaches the point where the system turns into a VDW. Meanwhile, U and G_2 do nothing: this is easily seen by adding and subtracting the first and the last lines of Eq. (19) $\dot{g}_U \pm \dot{g}_2 = -(g_U \pm g_2)^2$. This is just the lowest-order description of the real Cooper pairing instability in the s-wave spin-singlet channel with the superconducting gap parameter having either the same sign for both bands c and d (conventional s wave) or the opposite sign ($s_\pm$ wave or an extended

s wave, s'), the corresponding coupling constants being $g_U + g_2$ and $g_U - g_2$, respectively. Both of these coupling constants are repulsive and thus both scale toward zero and into the Fermi-liquid regime, leaving the VDW and W to determine the physics at low energies, *unless* $G_2 > U (\sim \sqrt{U_h U_e})$ at the *bare* level. This is not impossible but appears to be unlikely within the regime of interactions considered here, where G_2 is typically quite a bit smaller than U. This tells us that the direct coupling of G_2 to W's in the last line of Eq. (19) must be *crucial*: the growth of W's as we approach the VDW eventually pulls G_2 along with it while U still continues being renormalized downward. This growth of G_2 generated by its coupling to W's and the VDW could ultimately result in $G_2^\star > U^\star (\sim \sqrt{U_h^\star U_e^\star})$, where $G_2^\star$ and $U^\star$ are the renormalized coupling constants at some low energy scale $\omega_0 \ll \Lambda$, even though $G_2 < U (\sim \sqrt{U_h U_e})$ at the bare level. This implies that the coupling constant $g_U - g_2$ is *attractive* for $\omega < \omega_0$ and translates into growth of $s_\pm$ (s') pairing correlations at yet lower energies. All of this is for nothing, however, W's and the VDW instabilities are still far stronger. But, if the strong growth of W and the VDW instability are cut off by our fictitious Zeeman splitting in doped or pressurized FeAs (Fig. 1), then W stops growing at some energy scale $\omega_z \sim \delta\mu = \mu^e - \mu^h$ directly tied to the difference in FS size between h and e bands and the corresponding lack of perfect nesting. Then, if $\omega_z < \omega_0$, the subleading instability would take over and the ground state would be an $s_\pm$ (s') superconductor, either adjacent to the VDW boundary or coexisting with it in the pockets left ungapped by the VDW (Fig. 1). The above argument is similar in spirit to the weak-coupling mechanism for d-wave superconductivity once the single band repulsive Hubbard model is doped away from half filling and the SDW ground state. There is an important difference, however, if $\omega_z > \omega_0$ there will be no superconducting ground state since $g_U - g_2$ is still repulsive. This is a qualitative point and it underscores the fact that an $s_\pm$ (s') superconductor still has an overall s-wave symmetry and, unlike the nodal d wave, must contend with the strength of the bare intraband repulsion.

The second way is now obvious: G_2 enhancement near the VDW instability can overcome the repulsion U if an attractive intraband interaction is at work as well. Such intraband attraction might come from phonons, for example. This attraction may or may not suffice to produce superconductivity by itself—the key point is that it reduces the effective U's Eq. (17) allowing the enhanced G_2 to cross over the hurdle. Note that in both of these cases, the purely electronic and the phonon-assisted one, the superconducting gap on the hole and the electron portions of the FS will have the opposite sign,[6,18,27,29] reflecting the fact that the interband pairing term G_2 is repulsive.

V. CONCLUSIONS

In summary, we have proposed an idealized model of Fe pnictides which includes an electron and a hole band, and takes advantage of their similar shape and size. The ph transformation maps this model into a fictitious attractive Hubbard model in external "Zeeman" field. The ground states,

fictitious superconductor and the "FFLO" state, correspond to insulating and metallic VDW in real materials. Next, by considering deviations from perfect nesting, two hole and two electron bands, and other realistic features of Fe pnictides, we analyze the structure of interactions in the $8+8$ orbital model[18] and identify the interband pair resonance mechanism that can generate the real superconductivity in the region of the phase diagram of Fe pnictides where the VDW order gives way to strong VDW fluctuations.

[1] Y. Kamihara Hidenori Hiramatsu, Masahiro Hirano, Ryuto Kawamura, Hiroshi Yanagi, Toshio Kamiya, and Hideo Hosono, J. Am. Chem. Soc. **128**, 10012 (2006).

[2] Y. Kamihara, Takumi Watanabe, Masahiro Hirano, and Hideo Hosono, J. Am. Chem. Soc. **130**, 3296 (2008).

[3] X. H. Chen, T. Wu, G. Wu, R. H. Liu, H. Chen, and D. F. Fang, Nature (London) **453**, 761 (2008); G. F. Chen, Z. Li, D. Wu, G. Li, W. Z. Hu, J. Dong, P. Zheng, J. L. Luo, and N. L. Wang, Phys. Rev. Lett. **100**, 247002 (2008); Z.-A. Ren *et al.*, EPL **82**, 57002 (2008); Mater. Res. Innovations **12**, 105 (2008).

[4] See Physica C **469**, 313 (2009) for a comprehensive review of the current state of Fe-based superconductivity; in particular, A. V. Chubukov, *ibid.* **469**, 640 (2009); I. I. Mazin and J. Schmalian, *ibid.* **469**, 614 (2009) provide insightful accounts of the progress in theory.

[5] S. Lebègue, Phys. Rev. B **75**, 035110 (2007).

[6] I. I. Mazin, D. J. Singh, M. D. Johannes, and M. H. Du, Phys. Rev. Lett. **101**, 057003 (2008).

[7] C. Cao, P. J. Hirschfeld, and H.-P. Cheng, Phys. Rev. B **77**, 220506(R) (2008).

[8] R. T. Scalettar, E. Y. Loh, J. E. Gubernatis, A. Moreo, S. R. White, D. J. Scalapino, R. L. Sugar, and E. Dagotto, Phys. Rev. Lett. **62**, 1407 (1989); **63**, 218(E) (1989).

[9] T. M. Rice and B. I. Halperin, Phys. Rev. B **1**, 509 (1970).

[10] J. Froehlich, T. Chen, and M. Seifert, arXiv:cond-mat/9508063 (unpublished).

[11] C. de la Cruz *et al.*, Nature (London) **453**, 899 (2008); Y. Qiu *et al.*, Phys. Rev. Lett. **101**, 257002 (2008).

[12] Q. Huang, Y. Qiu, W. Bao, M. A. Green, J. W. Lynn, Y. C. Gasparovic, T. Wu, G. Wu, and X. H. Chen, Phys. Rev. Lett. **101**, 257003 (2008).

[13] K. E. Wagner *et al.*, Phys. Rev. B **78**, 104520 (2008); T. M. McQueen, A. Williams, P. Stephens, J. Tao, Y. Zhu, V. Ksenofontov, F. Casper, C. Felser, and R. Cava, arXiv:0905.1065 (unpublished).

[14] J. G. Analytis, R. McDonald, J. Chu, S. Riggs, A. Bangura, C. Kucharczyk, M. Johannes, and I. Fisher, arXiv:0902.1172 (unpublished).

[15] D. Bhoi, P. Mandal, and P. Choudhury, Physica C **468**, 2275 (2008).

[16] X. Yang, J. C. Davis, *et al.*, Nature (London) (to be published).

[17] K. Kuroki, S. Onari, R. Arita, H. Usui, Y. Tanaka, H. Kontani, and H. Aoki, Phys. Rev. Lett. **101**, 087004 (2008).

[18] V. Cvetkovic and Z. Tesanovic, EPL **85**, 37002 (2009).

[19] See G. A. Sawatzky, I. S. Elfimov, J. van den Brink, and J. Zaanen, EPL **86**, 17006 (2009).

[20] V. Cvetkovic and Z. Tesanovic (unpublished).

[21] For properties of FFLO states see H. Shimahara, Phys. Rev. B **62**, 3524 (2000); M. L. Kulic and U. Hofmann, Solid State Commun. **77**, 717 (1991), and references therein.

[22] A variety of lattice effects in real materials keep the modulation of VDW more strongly pinned to **M** than in the standard FFLO case (Ref. 21). Thus, it is useful to identify the FFLO state with the metallic VDW (Fig. 1). Alternatively, one could draw on the current language of cold atomic gases and reserve the label FFLO for the incommensurate metallic VDW while the commensurate metallic VDW in this nomenclature becomes a "breached pairing" fictitious superconductor.

[23] The introduction of the extra isospin flavor defines a minimal model within which all the interaction vertices are allowed to assume their local form. For example, the short-range on-site intraband (intraflavor) repulsion $U_{h(e)}$ does not enter within our elementary SU(2) model alone since $n_i^2 = n_i$ for fermion particle number operators. Of course, this is not a problem at all and one simply has to look at the nonlocal intraband repulsion and pairing terms for spinless fermions but this is not what will ultimately correspond to actual pnictides, where there are two extra pairs of flavors, additional orbital and the real spin, for the total of four, and the local interactions among these flavors is all that is needed.

[24] H. Suhl, B. T. Matthias, and L. R. Walker, Phys. Rev. Lett. **3**, 552 (1959).

[25] S. Raghu, X. L. Qi, C. X. Liu, D. J. Scalapino, S. C. Zhang, Phys. Rev. B **77**, 220503(R) (2008).

[26] Y. Ran, F. Wang, H. Zhai, A. Vishwanath, and D. H. Lee, Phys. Rev. B **79**, 014505 (2009).

[27] A. V. Chubukov, D. V. Efremov, and I. Eremin, Phys. Rev. B **78**, 134512 (2008).

[28] F. Wang, H. Zhai, Y. Ran, A. Vishwanath, and D. H. Lee, arXiv:0805.3343 (unpublished); Phys. Rev. Lett. **102**, 047005 (2009).

[29] M. M. Parish, J. Hu, and B. A. Bernevig, Phys. Rev. B **78**, 144514 (2008); K. Seo, B. A. Bernevig, and J. Hu, Phys. Rev. Lett. **101**, 206404 (2008).